Hindawi
Journal of Chemistry
Volume 2019, Article ID 4314975, 11 pages
https://doi.org/10.1155/2019/4314975

Research Article

Tuning Catalytic Properties of Supported Bimetallic Pd/Ir Systems in the Hydrogenation of Cinnamaldehyde by Using the "Water-in-Oil" Microemulsion Method

Tomasz Szumełda,[1] **Alicja Drelinkiewicz**,[1] **Francesco Mauriello**,[2] **Maria Grazia Musolino**,[2] **Anna Dziedzicka**,[1] **Dorota Duraczyńska**,[1] **and Jacek Gurgul**[1]

[1]*Jerzy Haber Institute of Catalysis and Surface Chemistry, Polish Academy of Sciences, Niezapominajek 8, 30-239 Krakow, Poland*
[2]*Dipartimento DICEAM, Università Mediterranea di Reggio Calabria, Loc. Feo di Vito, I-89122 Reggio Calabria, Italy*

Correspondence should be addressed to Tomasz Szumełda; ncszumel@cyfronet.pl and Francesco Mauriello; francesco.mauriello@unirc.it

Received 25 September 2018; Accepted 16 December 2018; Published 3 February 2019

Academic Editor: Bartolo Gabriele

Supported Pd/Ir bimetallic catalysts were synthesized by the "water-in-oil" microemulsion method at different precursor concentrations and characterized by XRD, XPS, SEM, TEM, and cyclic voltammetry. Depending on the preparation conditions, formation of bimetallic catalysts with different metal segregation and surface composition can be easily obtained, thus tuning the bimetallic structure of catalysts as well as their relative catalytic properties. Bimetallic Pd/Ir systems were efficiently tested in the hydrogenation of cinnamaldehyde showing a better performance than analogous monometallic catalysts.

1. Introduction

The synthetic procedure is surely one of the main key factors determining morphology and surface properties of heterogeneous catalysts [1]. In the last decades, a lot of attention has been addressed to the preparation of supported bimetallic systems [2–7] that, at present, represent one of the most important categories of heterogeneous catalysts being involved in many types of reactions including oxidation, hydrogenation, dehydrogenation, hydrogenolysis, aqueous phase reforming (APR), and H-transfer reactions [8–13]. In order to obtain bimetallic structures with a controlled surface composition, several synthetic methods have been proposed [11, 14–30]. Among the many known, the microemulsion (ME) synthesis method seems to be one of the most promising synthetic procedures for the preparation of bimetallic particles due to the possibility of controlling the particle size and the composition (alloy, core-shell, and enriched core/enriched shell) [28, 31, 32]. In the ME method, small amounts of an aqueous solution containing metal ions are added to the surfactant/oil phase system (micellar solution). Under these conditions, micelles are formed spontaneously and, by introducing a reducing agent, their nucleation is followed by the growth of the bimetallic particles [33]. Nevertheless, the final bimetallic structure is conditioned by many factors such as the composition of microemulsions [34], the type of precursor [20, 35], the difference of standard reduction potentials of metal ions (ΔE^0, V) [28, 36, 37], and the concentration of precursor solutions [36, 38, 39]. Many examples of bimetallic structures have been reported by using the microemulsion method including Pt/Ag [37], Pd/Ag [40], Au/Pt [38, 41, 42], Pd/Pt [43], Pd/Au [44, 45], Pd/Ni [46], Pt/Cu [47], and Pt/Co [48] systems. At present, there is still no insightful research available on Pd/Ir bimetallic structures obtained by the ME method. However, Pd/Ir systems are promising catalysts for hydrogenation [49], reduction [50] oxidation, and electro-oxidation [51–53] reactions. A synergy between Pd and Ir has been reported by Nakagawa et al. [54] in the silica-supported PdIr (1 : 1) alloy particles in the total hydrogenation of furfural. Accordingly, Zlotea et al. [55] reported that the catalytic performance of the CO oxidation

could be enhanced when Ir is added to Pd. A significant promotion of Pd by Ir in nitrobenzene hydrogenation has been reported by Yang et al. [56] in mesoporous silica supporting Pd/Ir catalysts where the promotional effect of Ir has been related to its interaction with Pd and the consequent charge transfer from Ir to Pd. Some of the authors report that despite the large difference of reduction potentials (Ir = 1.19 V; Pd = 0.48 V), PdIr particles (Pd/Ir molar ratio = 10) of almost homogeneous alloy microstructure can be formed by using the ME method. Moreover, Ir has a higher surface energy and heat of sublimation (3.00 J/m^2 and 195 kJ/mol, respectively), and the values are higher than those of Pd (2.05 J/m^2 and 136 kJ/mol, respectively) [57, 58]. Both values lead to core-shell structure formation, with the core enriched in Ir and the shell enriched in Pd [17].

In the present work, supported (carbon and SiO_2) Pd/Ir bimetallic catalysts are synthesized by the ME method with a $Pd_{74}Ir_{26}$ atomic ratio. Their morphological and structural characteristics were determined by XRD, XPS, and electron microscopy (SEM and TEM). Surface properties of PdIr particles, including Pd and Ir surface fractions, and the hydrogen sorption/desorption ability were characterized by means of cyclic voltammetry (CV) measurements. Catalytic tests were performed to gain more insights into Pd/Ir surface properties, taking into account, in particular, the role of Ir in promoting the modification of Pd reactivity. The hydrogenation of cinnamaldehyde was chosen as a model reaction, highlighting the properties of the catalyst surface, such as the distribution/type of the bimetallic structure as well as its role in the activity/selectivity pattern [59–62].

2. Materials and Methods

2.1. Catalysts Preparation. Unless otherwise specified, all reagents were purchased from Sigma-Aldrich. Carbon (Vulcan XC72, CABOT) and silica (Davisil 634) were used as supports. The monometallic Pd and Ir catalysts (2 wt.% metal loading) and the bimetallic Pd/Ir systems (2 wt.% of Pd metal and 1.3 wt.% of Ir metal loading) were prepared by the reverse "water-in-oil" microemulsion method as previously described [22, 55]. Polyoxyethylene (78) and octylphenylether (Triton-X 114) were used as surfactants and cyclohexane as the organic solvent, and the $W = 5.5$ was kept as the molar ratio of water/surfactant. The 0.02, 0.04, 0.08, 0.14, and 0.2 M aqueous solutions of $IrCl_3$ were prepared by using a commercial reagent. The precursor solutions of Pd^{2+} ($PdCl_2$) ions at different concentrations 0.02, 0.04, 0.08, 0.14, and 0.2 M were prepared using NaCl (dried at 120°C) at a molar ratio of NaCl : $PdCl_2 = 2$. The synthesis of 0.5 g of 2% Pd/C and 0.5 g of 2% Pd/SiO_2 was carried out as follows: 0.94 cm^3 of a 0.2 M solution containing Pd^{2+} ions and 16.8 cm^3 of a cyclohexane solution of the surfactant (0.62 M) were stirred until the microemulsion was transparent. Then, $NaBH_4$ (in a 10 : 1 molar ratio of reducing agent/metal ions) was added and the stirring was continued for another hour. The microemulsion was then divided into two parts, and 0.49 g of each support (carbon or SiO_2) was added under stirring for another hour. The deposition of metal particles on the supports was made by introducing the THF solvent. The ratio of the volume of added THF to the volume of the microemulsion was 3 : 1. Finally, the catalysts were filtered, washed with acetone, and dried.

All PdIr supported catalysts were synthesized using a total metal loading of 3.3 wt.% (Pd + Ir) and a Pd : Ir atomic ratio of 74 : 26 ($Pd_{74}Ir_{26}$). During the preparation, a mixture of $PdCl_4^{2-}$ and $IrCl_3$ solutions having different molar concentrations and cyclohexane as well as surfactant were mixed.

2.2. Catalysts Characterization. XRD patterns were measured with a Philips X'PERT diffractometer using Cu Kα radiation (40 kV, 30 mA).

XPS measurements were carried out with a hemispherical analyzer (SES R4000, Gammadata Scienta).

SEM studies were performed with a field emission scanning electron microscope (JEOL JSM–7500 F) equipped with the X-ray energy dispersive system (EDS).

TEM studies were performed on an FEI Tecnai G2 transmission electron microscope operating at 200 kV equipped with EDX analysis.

The cyclic voltammetry (CV) measurements were made by using a CH Instrument (Austin, TX, USA) Model CHI760D workstation with a scan rate of 50 mV using a 0.5 M solution of H_2SO_4.

2.3. Catalytic Tests. Catalytic reactions were performed in a batch glass reactor at a temperature of 50°C and a constant atmospheric pressure of hydrogen (20 cm^3 of a cinnamaldehyde solution in toluene having 0.05 mol/dm^3 of c_0 and 5 g/dm^3 of catalysts was used). The methodology has been described in detail previously [22, 55]. In all hydrogenation reactions, silica-supported catalysts were employed in order to exclude the fact that the electronic properties of the carbon support may influence the activity/selectivity of samples, so that the catalytic properties only derive from those of the system [63].

The catalyst and the solution were put in the reactor without addition of reagents in order to allow the in situ catalyst activation by hydrogen at a temperature of 50°C before the hydrogenation test. Then, the catalyst was mixed with the reagent solution and the experiment started. The progress of the reaction was measured from the consumption of hydrogen. Samples were withdrawn from the reactor via a tube at intervals of time and analyzed by GC.

3. Results and Discussion

3.1. Physicochemical Characterization of Bimetallic Structure of Supported Pd/Ir Catalysts. XRD patterns of Ir/SiO_2, Pd/SiO_2, and PdIr-0.2/SiO_2 catalysts are shown in Figure 1. The Pd/SiO_2 diffraction peaks at about $2\theta = 40°$, 46°, 68°, and 82° can be assigned to Pd (111), (200), (220), and (311) crystal planes, respectively, which indicate a typical cubic crystal (fcc) structure of Pd [64]. The crystalline Ir also has an fcc structure, but no Ir diffraction peaks were observed in the 2% Ir/SiO_2 system. This may be caused by the low Ir loading, the amorphous distribution of the metal, or the presence of small crystallites of iridium. In addition, on analyzing the

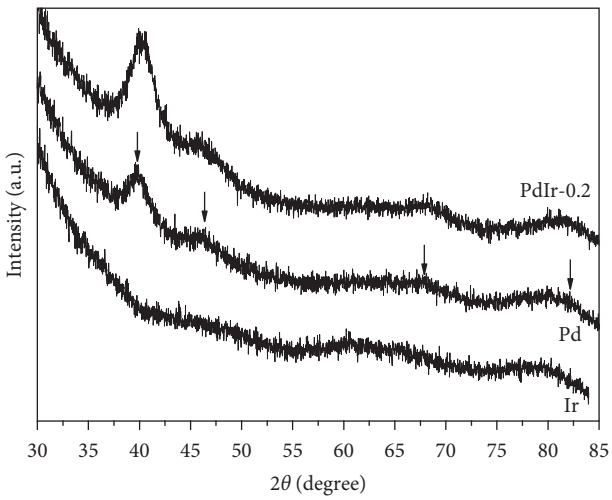

Figure 1: XRD diffraction patterns of Ir/SiO_2, Pd/SiO_2, and PdIr-$0.2/SiO_2$.

PdIr-$0.2/SiO_2$ catalyst, four diffraction peaks were detected at higher 2θ values compared to those of Pd/SiO_2. This may be related to the presence of a crystalline structure with a lower d space relative to Ir species ($d_{111} = 2.217$) compared with that of Pd ($d_{111} = 2.246$) and the subsequent formation of a Pd-Ir alloy [65].

Accordingly, peaks of PdIr-0.02, PdIr-0.04, PdIr-0.08, PdIr-0.14, and PdIr-0.2 are presented in Figure 2, and it can be observed that the one peak located around $2\theta = 40^\circ$ is slightly shifted toward higher 2θ values with respect to that of Pd/SiO_2, indicating that some Ir atoms enter the Pd lattice, forming a PdIr alloy as well. Reduced lattice parameters in all PdIr crystallites (Table 1) compared to those of pure Pd confirm a PdIr alloy formation [66]. Moreover, the shift differences in all PdIr catalysts may indicate a different surface and volume composition, related to the amount of Ir incorporated into Pd. This effect may depend on the concentration used in the precursor synthesis. In all XRD patterns, peak characteristics of IrO_2, $2\theta = 34.5^\circ$ and 54°, were not observed [67]. The average crystallite sizes of all prepared catalysts were estimated using the Scherrer equation [68] and are presented in Table 1. PdIr catalysts have a smaller particle size than the monometallic Pd.

SEM images indicate that, for PdIr bimetallic catalysts, particles are almost dispersed over the support (Figure 3). However, on increasing the concentration of precursors, more aggregates are visible, as confirmed by the TEM analysis. A similar effect was also observed by Liz-Marzán and Lado-Touriño [70] during the formation of Ag nanoparticles: when the $AgNO_3$ concentration rises, the mean diameter of silver nanoparticles decreases if $AgNO_3 \leq 0.2$ M and increases if $AgNO_3 > 0.2$ M. At a higher concentration, silver nanoparticles begin to aggregate and form large particles. This phenomenon has been explained by considering the formation of a large number of silver nanoparticles at a higher concentration of $AgNO_3$. As a result, the collision frequency increases significantly, and this neutralizes the surfactant molecules' protective effect and results in a higher aggregation.

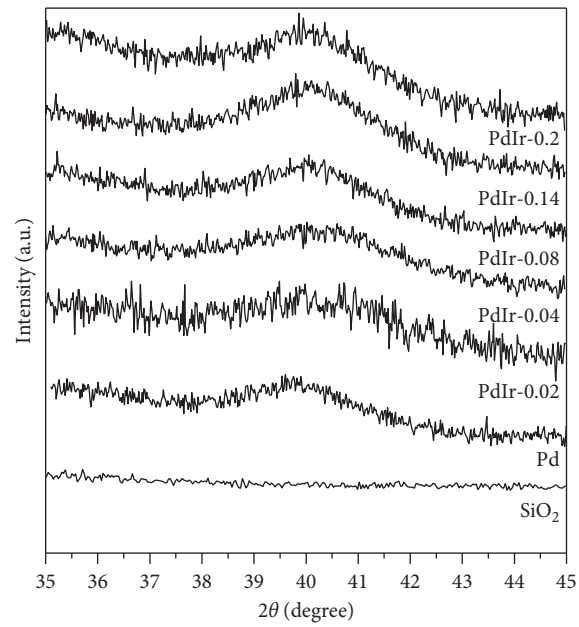

Figure 2: XRD diffraction patterns of silica-supported PdIr-0.02, PdIr-0.04, PdIr-0.08, PdIr-0.14, and PdIr-0.2 catalysts.

Particles size distribution, as determined by the TEM analysis, indicates a narrow range of 2–7 nm and the average particles size was calculated by counting over 100 particles for each catalyst (Figure 4). It can be observed that as the concentration of the precursor increases, a very slight particle-size increase is noticed: PdIr-0.02 (4.4 nm), PdIr-0.08 (4.5 nm), and PdIr-0.2 (4.8 nm), and it should be pointed out that the average size of the metal particles, calculated from the microscopic images, is consistent with the XRD results. Comparing these data with the particles size of Pd (6.0 nm) and Ir (4.2 nm) monometallic particles [69], it can be inferred that after addition of Ir, the size of bimetallic particles decreases and reaches the value close to that characteristic of Ir. This metal-type particle-size effect is the result of the main role of the nucleation process, being decisive for the particles' formation in the microemulsion medium. The nucleation process is determined by the metal properties, namely, the heat of metal vaporization ΔH_{VAP} (or sublimation, ΔH_S) that determines the strength of the (M-M) metal-metal bond and the size of the critical nucleus, in accordance with previous results concerning interactions of Ir with Pt and Rh with Pd [71]. The Pd/Ir atomic ratio, determined by EDS analysis (Table 1), confirms the presence of both Pd and Ir metals in the nanoparticles in agreement with the nominal composition.

The catalysts were also examined by X-ray photoelectron spectroscopy (XPS) experiments. The surface composition of Pd and Ir (in at.%) and the binding energies of palladium Pd $3d_{5/2}$ and Ir $4f_{7/2}$ peaks are included in Table 2.

The binding energy of Pd $3d_{5/2}$ in all PdIr catalysts is slightly shifted to a higher energy value compared to the metallic state of Pd (335.3 eV) [44]. PdIr-0.02 shows the largest binding energy shift $\Delta E = 0.5$ eV, while in other PdIr catalysts ΔE values are in a range of 0.1–0.4 eV. The larger shift of the binding energy for the PdIr-0.02 system can be

Table 1: Physicochemical properties of investigated catalysts: metal particle characterization (average size, the overall composition measured by EDS, and the local composition measured by STEM-EDX methods) and the initial rate of cinnamaldehyde hydrogenation.

Catalyst	Metal particle size d (nm)		Lattice parameter (Å)	Pd : Ir atomic ratio		Initial rate R ($mol\cdot_{CAL}10^{-5}\cdot min^{-1}\cdot g\ (cat)^{-1}$)	TOF (s^{-1})
	XRD	SEM/TEM		EDS	STEM-EDX		
Pd	6.0 ± 0.5	6.0 ± 0.5*	3.906	—	—	24.4	0.121
PdIr-0.02	4.3 ± 0.5	4.4 ± 0.5	3.883	77 : 23	75 : 25	46.0	0.138
PdIr-0.04	4.4 ± 0.5	—	3.883	—	—	31.5	0.091
PdIr-0.08	4.5 ± 0.5	4.5 ± 0.5	3.884	74 : 26	72 : 28	14.0	0.042
PdIr-0.14	4.6 ± 0.5	—	3.884	—	—	10.1	0.031
PdIr-0.2	4.9 ± 0.5	4.8 ± 0.5	3.885	78 : 22	73 : 27	7.4	0.024
Ir	—	4.2 ± 0.5*	3.840**	—	—	—	—

*Reference [69]; **Reference [51].

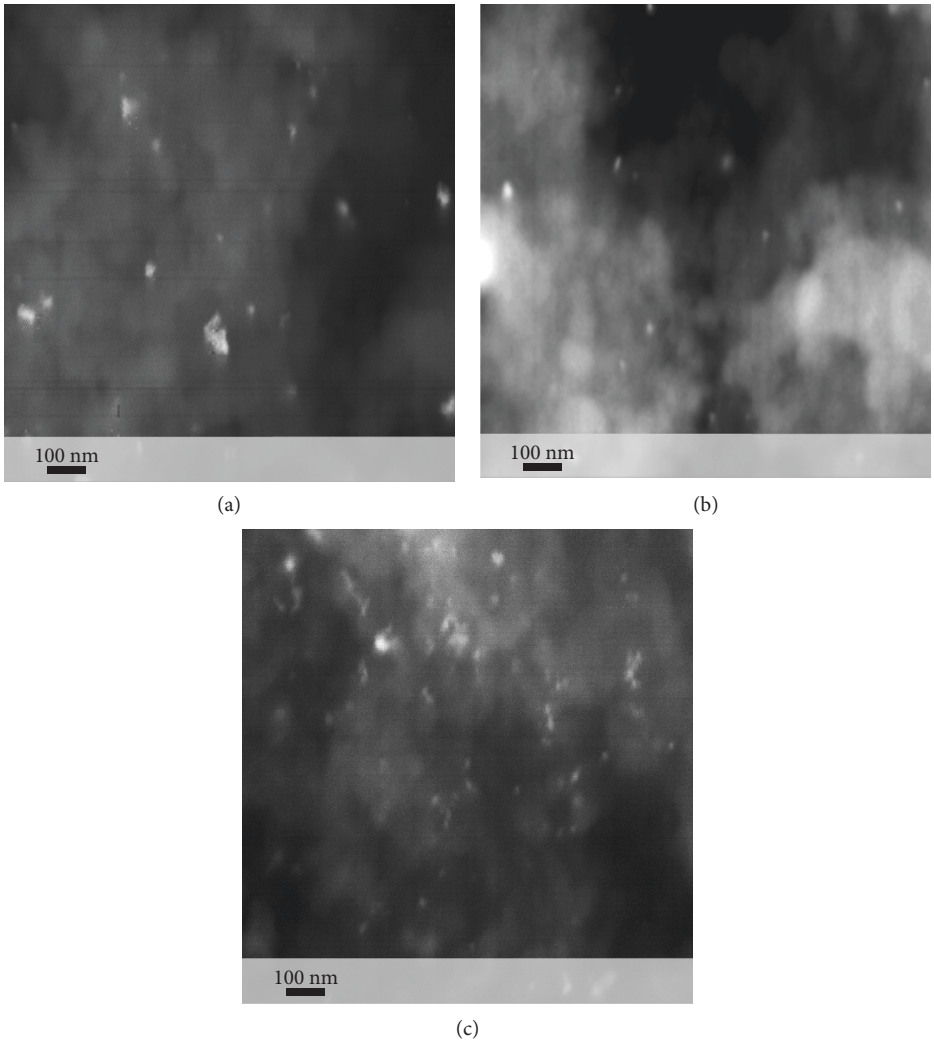

Figure 3: SEM images (magnification 100 000) of bimetallic (a) PdIr-0.02/C, (b) PdIr-0.08/C, and (c) PdIr-0.2/C catalysts.

ascribed to the strongest surface electronic modification of the Pd derived from its interaction with Ir [53]. The presence of Ir on the surface of bimetallic particles is also observed in all catalysts. In the PdIr-0.02 system, the atomic ratio, Pd to Ir (1.95/1.03), is 1.89, while in the PdIr-0.2, it is close to 1, suggesting a stronger surface enrichment in Ir atoms compared to that in the PdIr-0.02, obtained from the most diluted precursor. Nevertheless, the electron modification of the PdIr-0.02 catalyst is more pronounced (BE shift = 0.5 eV). This effect may suggest a stronger dispersion of Ir on the surface, which results in a stronger modification of Pd in the presence of the more dispersed Ir.

The catalysts were also characterized by cyclic voltammetry (CV) in order to examine more accurately the structure of bimetallic particles. Voltammograms, recorded for all catalysts, are shown in Figure 5.

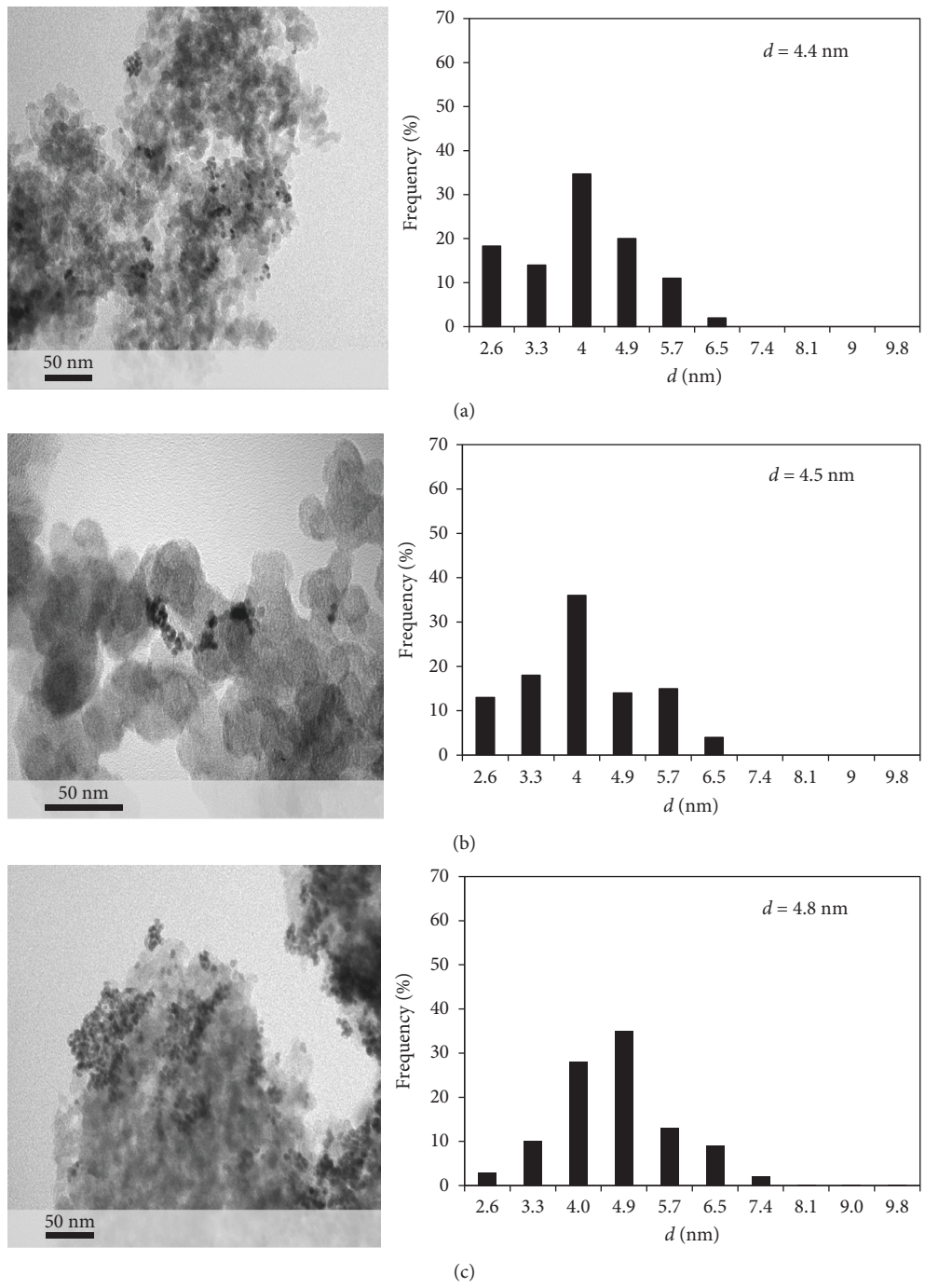

Figure 4: TEM micrographs of bimetallic (a) PdIr-0.02/C, (b) PdIr-0.08/C, and (c) PdIr-0.2/C catalysts with the corresponding particle-size distribution diagrams.

Table 2: XPS data and surface fraction of Pd and Ir components determined by CV measurements.

Catalyst	XPS data					Surface fraction (CV)	
	Pd (at.%)	Ir (at.%)	Pd $3d_{5/2}$ BE (eV)	BE shift (eV)	Ir $4f_{7/2}$ BE (eV)	Pd	Ir
Pd	—	—	335.3	—	—	1	
PdIr-0.02	1.95	1.03	335.8	0.5	61.7	0.85	0.15
PdIr-0.04	—	—	—	—	—	0.83	0.17
PdIr-0.08	1.33	0.86	335.4	0.1	60.9	0.81	0.19
PdIr-0.14	1.04	0.75	335.5	0.2	61.0	0.80	0.20
PdIr-0.2	0.71	0.74	335.7	0.4	61.2	0.77	0.23
Ir	—	—	—	—	60.7		1

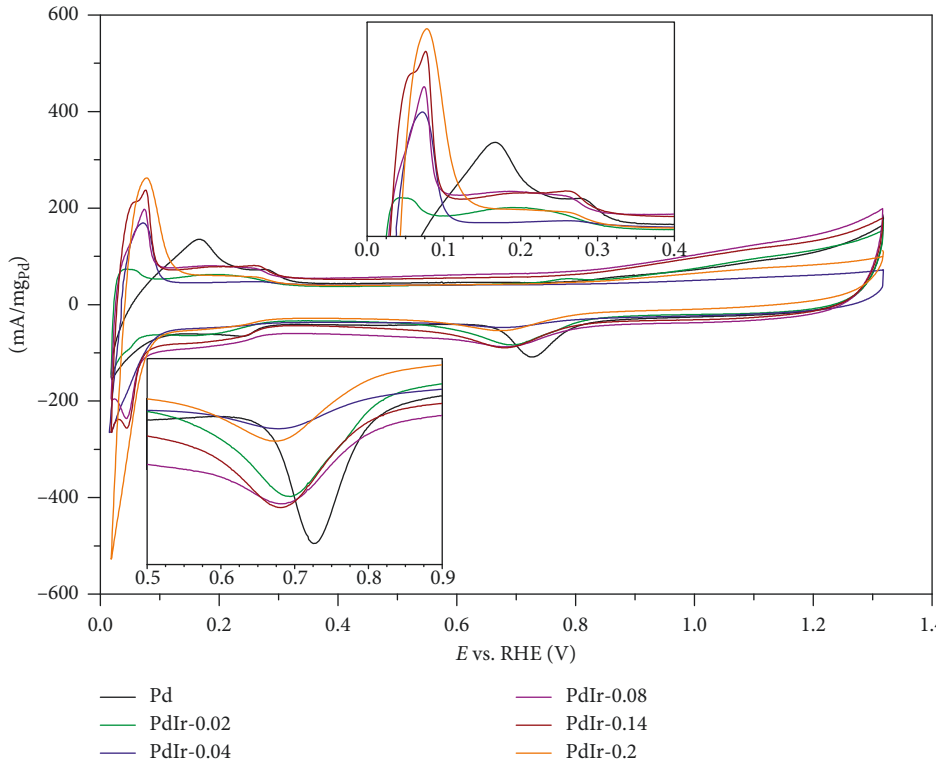

Figure 5: Cyclic voltammograms for mono Pd and bimetallic PdIr catalysts in N_2-saturated 0.5 M H_2SO_4 solution with a scan rate of 50 mV/s. The insets are magnified views of the hydrogen desorption region (0.0–0.4 V) and the metal surface reduction region (0.5–0.9 V).

Peaks corresponding to adsorption and desorption of hydrogen are clearly detected in bimetallic systems together with a shift of the hydrogen desorption component (magnification, area A of Figure 5) towards lower potentials for all studied catalysts compared to pure Pd samples. Chen et al. [52] attributed the effect of the negative hydrogen desorption peak shift to the weakened adsorption energy of hydrogen. This is a consequence of the downshift of the Pd *d*-band centre related to the presence of Ir on both the surface and the bulk of the bimetallic structure. The shape of hydrogen desorption peaks is also changing, and this confirms the modification of the Pd electronic properties by adding Ir [51, 72–74]. Therefore, it can be assumed that, in each of the investigated catalysts, Ir is present on the surface of PdIr bimetallic particles, affecting the Pd-Ir interaction and thus influencing the degree of coverage by hydrogen in the surface. The presence of the second metal on the surface, as well as the electron interaction between both components, was also confirmed by XPS studies.

For the Pd catalysts, a reduction peak of PdO is observed at the potential of $E = 0.727$ V and this is consistent with the reduction of surface-oxidized Pd(II) species [75, 76]. For all PdIr catalysts, only one reduction peak of oxidized forms of metals is visible, having a different potential than that of Pd/C. Curves relative to PdIr catalysts do not show separate peak characteristic of separate reduction of oxidized forms of Pd and Ir, indicating the homogeneity of the alloy surface composition [77].

The surface composition of bimetallic particles (Pd and Ir surface fraction) was calculated from formula (1), including the linear correlation between the peak reduction potential and the surface composition ($E_{P,Pd}$, $E_{P,Ir}$ are oxide reduction peak potentials for pure Pd (0.727 V) and Ir (0.505 V), and X_{Pd} and X_{Ir} are surface fractions of Pd and M) [77]:

$$E_{P,ALLOY} = X_{Pd} \times E_{P,Pd} + X_{Ir} \times E_{P,Ir}. \quad (1)$$

This method was, so far, used by many authors for the analysis of bimetallic films, as well as for the determination of the surface composition of particles in PdPt/C, PdAu/C, PdIr/C, and PdPtAu/C catalysts [69, 78, 79]. Surface fractions of Ir and Pd calculated from equation (1) are summarized in Table 2.

For all catalysts, the surface fraction of Ir is smaller (0.15–0.23) than that of the bulk composition (0.26 for the $Pd_{74}Ir_{26}$ sample), indicating the palladium enrichment of the surface and the segregation of Ir in the core of particles. Nevertheless, the effect of the surface increase of iridium on increasing the precursor concentration is evident. The lowest surface fraction is observed in the case of the PdIr-0.02 catalyst, while for the catalyst synthesized from the precursor solution with the highest concentration (PdIr-0.2), the surface composition of Ir is almost the same as that of the bulk composition (0.23). Moreover, by analyzing the hydrogen desorption peak shapes (Figure 4, area A) of the catalysts, it can be concluded that for those systems, obtained from the precursor having the lowest concentration (PdIr-0.02), the shape significantly differs than those in catalysts obtained from precursors with higher concentrations (PdIr-0.04, PdIr-0.08, PdIr-0.14, and PdIr-0.2). This may indicate

that there is a different distribution (mixing in atomic-level alloy, nonatomic alloy, and atomic clusters) of Ir on the surface of bimetallic structures and that there are possible different interactions of Pd-Ir.

Monte Carlo simulations [80, 81] and experimental works [38, 44, 47, 82] have also shown that the difference in the reduction potential of precursor ions, in the w/o microemulsion, may affect the type of bimetallic structures (core-shell, alloy, and cluster in cluster). In general, the higher is the difference in reduction potentials, the stronger is the segregation of metals and formation of core-shell structures is observed. It has been also reported that the resulting bimetallic arrangement reflects the combination of two potentially limiting factors: the reduction rate of each metal ion and the intermicellar exchange rate [83]. Reduction potentials relative to 0.2 M $PdCl_4^{2-}$ and $IrCl_3$ precursor concentrations have been previously determined by the linear voltammetry [69], exhibiting a significant difference ($\Delta E > 0.7$ V). According to the literature, formation of core (Ir)-shell (Pd) structures is the most probable. Data relative to all bimetallic PdIr catalysts show that the structures are similar to those having an incomplete core-shell structure. Therefore, it can be concluded that the difference in reduction potentials is not the only decisive factor for the type of bimetallic structure formed following the w/o microemulsion route. Monte Carlo simulations reveal, in fact, that differences in nucleation and growth can also influence the resulting structures [84]. Calculations show that in the case of heterogeneous nucleation, when the nucleation process is decisive, smaller heterogeneous critical nuclei compared to the homogeneous ones should prefer the final particles to form an alloy structure. They also demonstrate that when the formation of heterogeneous nuclei is faster than the homogeneous nucleation, the degree of metal components alloying in the final particles is greater. It can therefore be suggested that, by changing the concentration of the precursor solutions, the nucleation processes may be "modified" and play a more decisive role in comparison to the processes resulting from the difference in reduction potentials.

3.2. Catalytic Hydrogenation of Cinnamaldehyde. In order to verify the effect of both different iridium surface fraction and distribution, the catalytic hydrogenation of cinnamaldehyde was carried out. Simplified possible cinnamaldehyde hydrogenation pathways are presented in Scheme 1.

The catalytic test shows that hydrogenation of cinnamaldehyde leads to hydrocinnamaldehyde (HCAL), cinnamyl alcohol (COL), and the corresponding saturated alcohol (HCOL). β-Methyl styrene and phenyl propane have not been detected under the reaction conditions adopted. It is known that Pd is active and very selective towards C=C hydrogenation [85]. Ir is much less active and generally selective towards C=O hydrogenation [86]. In addition, monometallic Ir does not exhibit any observable activity relative to CAL hydrogenation under the studied reaction conditions. The activity relative to all catalysts is expressed by the initial rate of hydrogenation (R, related to the catalyst mass) and TOF (s^{-1}) values calculated with the formula given by Long et al. [87]. Results are reported in Table 1: the highest TOF value (Figure 6) belongs to the PdIr-0.02 catalyst ($0.138\,s^{-1}$) that is higher than the one relative to the monometallic Pd catalyst ($0.121\,s^{-1}$). Under the adopted reaction condition, no catalytic activity of the monometallic Ir catalyst was observed.

Furthermore, the activity decreases on increasing the precursor concentration used in the synthesis, as inferred from the highest TOF value, detected for the sample PdIr-0.02 ($0.138\,s^{-1}$) compared to the lowest one, calculated for the PdIr-0.2 catalyst ($0.024\,s^{-1}$). All bimetallic catalysts, except PdIr-0.02, exhibit also a minor activity than the monometallic Pd catalyst. Yang et al. [56] observed a strong increase of the activity in the hydrogenation of nitrobenzene in the presence of Pd catalysts after the addition of small amounts of Ir (Pd/Ir molar ratio of 0.1). This was explained by the size decrease of bimetallic particles and the simultaneous increase of both active sites and Pd electron modifications in the presence of Ir. In our catalytic systems, it can be suggested that the effect of the particle size on the activity and selectivity can be excluded as all PdIr particles, regardless of the concentration, are in a similar, very narrow size range (4.4–4.9 nm) [56]. Moreover, the effect of the surface metal composition on the selectivity of the CAL hydrogenation is reported in Figure 6 and shows the selectivity to the saturated alcohol (HCOL) obtained at 80% CAL conversion. The monometallic Pd catalyst has a selectivity to HCOL of around 12%. Of all the bimetallic catalysts examined, the PdIr-0.02 catalyst exhibits the highest selectivity towards the C=O hydrogenation (about 35%), which is nearly three times higher than the one calculated with the monometallic Pd. It can also be observed that as the concentration of the precursor used in the synthesis increases, the selectivity to HCOL decreases and is about 18% on using the PdIr-0.2. A remarkable PdIr synergy has been observed also by Nakagawa et al. [54] in the silica-supported Pd-Ir (1/1) alloy particles in the total hydrogenation of furfural. The activity/selectivity enhancement of active sites formed in the PdIr alloys has been related to the presence of Ir that may promote the adsorption of C=O of furfural accompanied by a weaker adsorption of the furan ring.

In our catalytic systems, it can be suggested that differences in both activity and selectivity may result from a different promotional effect of Ir, which, in turns, depends on the surface architecture of the PdIr species. There is, in fact, a clear tendency of the surface growth of the Ir fraction from 0.15 to 0.23 with the increasing concentration of the precursor solution (CV studies). Furthermore, in all PdIr catalysts, Ir is present on the surface; however, in the catalyst obtained from the lowest precursor concentration, the fraction of Ir is the lowest. Analogous results were also obtained with Monte Carlo simulations given by Tojo et al. [88], where the precursor concentration influence (0.01 M–0.40 M) on the bimetallic Au/Pt structure was studied, showing, theoretically, that the higher concentration of precursor with a faster reduction rate should afford a better core-shell structure. In our PdIr catalysts,

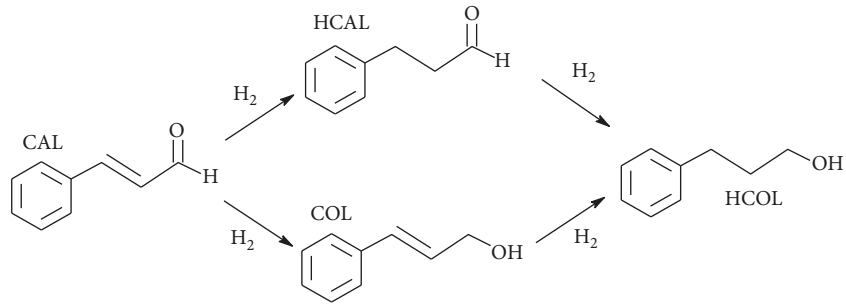

Scheme 1: Possible ways for the hydrogenation of cinnamaldehyde (CAL).

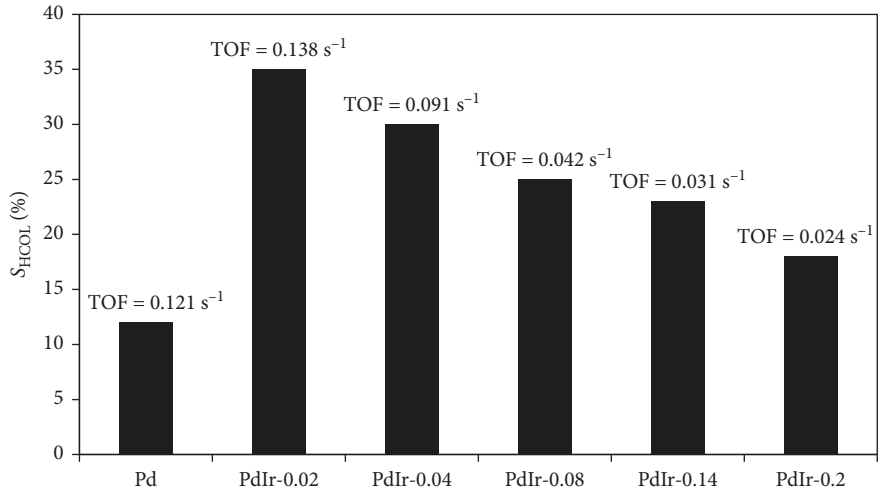

Figure 6: Selectivity to saturated alcohol (HCOL) obtained at 80% conversion of CAL with the TOF values for Pd and PdIr catalysts.

Ir is present on the surface and for the one obtained from the lowest precursor concentration, the fraction of Ir on the surface is the lowest. Moreover, it has also to be pointed out that, on using 0.02 M–0.2 M precursor concentrations, a complete core (Ir)-shell (Pd) structure is not obtained. Therefore, Ir is the most dispersed on the surface of bimetallic particles synthesized from the 0.02 M precursor (PdIr-0.02), and this results in a strong Pd-electron modification (XPS studies). On the other hand, a strong decrease in activity, on increasing precursor concentrations, may both be derived from increasing the surface area of Ir or/and a weaker dispersion of Ir (formation of clusters on the surface) compared to Pd. This may result in a weaker electron modification of Pd (XPS studies) and smaller number of available Pd active centres.

4. Conclusions

Supported PdIr bimetallic catalysts were synthesized by the "water-in-oil" microemulsion method with different precursor concentrations. The concentration of the precursor solutions (0.02 M, 0.04 M, 0.08 M, 0.14 M, and 0.2 M) has a significant influence on the type of PdIr bimetallic particles. XRD, TEM, and cyclic voltammetry (CV) studies confirm the formation of bimetallic structures containing Pd and Ir with different Ir fractions on the surface. For the PdIr-0.02 catalyst obtained from the most diluted precursor solution (0.02 M), the highest activity in the hydrogenation of cinnamaldehyde and the highest selectivity in the hydrogenation of the C=O bond were demonstrated. It can therefore be concluded that not only the difference in reduction rates of both metals but also synthesis conditions may play an important role in the process of nucleation, growth, and formation of bimetallic particles.

Data Availability

The data used to support the findings of this study are included within the article. Other data are available from the corresponding author upon request.

Conflicts of Interest

The authors declare that there are no conflicts of interest.

Acknowledgments

T. S. acknowledges financial support received under the action *Funds for Young Researchers* organized by the Director of Jerzy Haber Institute of Catalysis and Surface Chemistry, Polish Academy of Sciences.

References

[1] C. Perego and P. Villa, "Catalyst preparation methods," *Catalysis Today*, vol. 34, no. 3-4, pp. 281–305, 1997.

[2] E. Paone, C. Espro, R. Pietropaolo, and F. Mauriello, "Selective arene production from transfer hydrogenolysis of benzyl phenyl ether promoted by a co-precipitated Pd/Fe_3O_4 catalyst," *Catalysis Science & Technology*, vol. 6, no. 22, pp. 7937–7941, 2016.

[3] C. Espro, B. Gumina, E. Paone, and F. Mauriello, "Upgrading lignocellulosic biomasses: hydrogenolysis of platform derived molecules promoted by heterogeneous Pd-Fe catalysts," *Catalysts*, vol. 7, no. 12, p. 78, 2017.

[4] M. G. Musolino, L. A. Scarpino, F. Mauriello, and R. Pietropaolo, "Selective transfer hydrogenolysis of glycerol promoted by palladium catalysts in absence of hydrogen," *Green Chemistry*, vol. 11, no. 10, pp. 1511–1513, 2009.

[5] F. Mauriello, E. Paone, R. Pietropaolo, A. M. Balu, and R. Luque, "Catalytic transfer hydrogenolysis of lignin-derived aromatic ethers promoted by bimetallic Pd/Ni systems," *ACS Sustainable Chemistry & Engineering*, vol. 6, no. 7, pp. 9269–9276, 2018.

[6] M. Lo Faro, P. Frontera, P. Antonucci, and A. S. Aricò, "Ni-Cu based catalysts prepared by two different methods and their catalytic activity toward the ATR of methane," *Chemical Engineering Research and Design*, vol. 93, pp. 269–277, 2015.

[7] M. Boaro, V. Modafferi, A. Pappacena et al., "Comparison between Ni-Rh/gadolinia doped ceria catalysts in reforming of propane for anode implementations in intermediate solid oxide fuel cells," *Journal of Power Sources*, vol. 195, no. 2, pp. 649–661, 2010.

[8] M. Englisch, V. S. Ranade, and J. A. Lercher, "Liquid phase hydrogenation of crotonaldehyde over Pt/SiO_2 catalysts," *Applied Catalysis A: General*, vol. 163, no. 1-2, pp. 111–122, 1997.

[9] T. Szumełda, A. Drelinkiewicz, E. Lalik, R. Kosydar, D. Duraczyńska, and J. Gurgul, "Carbon-supported $Pd_{100-X}Au_X$ alloy nanoparticles for the electrocatalytic oxidation of formic acid: influence of metal particles composition on activity enhancement," *Applied Catalysis B: Environmental*, vol. 221, pp. 393–405, 2018.

[10] M. G. Musolino, C. V. Caia, F. Mauriello, and R. Pietropaolo, "Hydrogenation versus isomerization in the reaction of cis-2-butene-1,4-diol over supported catalysts: the role of Group VIII transition metals in driving the products selectivity," *Applied Catalysis A: General*, vol. 390, no. 1-2, pp. 141–147, 2010.

[11] E. Lalik, R. Kosydar, R. Tokarz-Sobieraj et al., "Humidity induced deactivation of Al_2O_3 and SiO_2 supported Pd, Pt, Pd-Pt catalysts in $H_2 + O_2$ recombination reaction: the catalytic, microcalorimetric and DFT studies," *Applied Catalysis A: General*, vol. 501, pp. 27–40, 2015.

[12] C. Espro, B. Gumina, T. Szumelda, E. Paone, and F. Mauriello, "Catalytic transfer hydrogenolysis as an effective tool for the reductive upgrading of cellulose, hemicellulose, lignin, and their derived molecules," *Catalysts*, vol. 8, no. 8, p. 313, 2018.

[13] D. Cozzula, A. Vinci, F. Mauriello, R. Pietropaolo, and T. E. Müller, "Directing the cleavage of ester C–O bonds by controlling the hydrogen availability on the surface of coprecipitated Pd/Fe_3O_4," *ChemCatChem*, vol. 8, pp. 1515–1522, 2016.

[14] Z. Xu, Y. Hou, and S. Sun, "Magnetic core/shell Fe_3O_4/Au and Fe_3O_4/Au/Ag nanoparticles with tunable plasmonic properties," *Journal of the American Chemical Society*, vol. 129, no. 28, pp. 8698-8699, 2007.

[15] C. Wang, H. Xu, R. Daniel et al., "Combustion characteristics and emissions of 2-methylfuran compared to 2,5-dimethylfuran, gasoline and ethanol in a DISI engine," *Fuel*, vol. 103, pp. 200–211, 2013.

[16] X. Gu, Z.-H. Lu, H.-L. Jiang, T. Akita, and Q. Xu, "Synergistic catalysis of metal-organic framework-immobilized Au-Pd nanoparticles in dehydrogenation of formic acid for chemical hydrogen storage," *Journal of the American Chemical Society*, vol. 133, no. 31, pp. 11822–11825, 2011.

[17] R. Ferrando, J. Jellinek, and R. L. Johnston, "Nanoalloys: from theory to applications of alloy clusters and nanoparticles," *Chemical Reviews*, vol. 108, no. 3, pp. 845–910, 2008.

[18] U. Kolb, S. A. Quaiser, M. Winter, and M. T. Reetz, "Investigation of tetraalkylammonium bromide stabilized palladium/platinum bimetallic clusters using extended X-ray absorption fine structure spectroscopy," *Chemistry of Materials*, vol. 8, no. 8, pp. 1889–1894, 1996.

[19] A. Y. Shenouda and E. S. M. El Sayed, "Electrodeposition, characterization and photo electrochemical properties of CdSe and CdTe," *Ain Shams Engineering Journal*, vol. 6, no. 1, pp. 341–346, 2015.

[20] D. V. Goia and E. Matijević, "Preparation of monodispersed metal particles," *New Journal of Chemistry*, vol. 22, no. 11, pp. 1203–1215, 1998.

[21] N. Toshima and T. Yonezawa, "Bimetallic nanoparticles-novel materials for chemical and physical applications," *New Journal of Chemistry*, vol. 22, no. 11, pp. 1179–1201, 1998.

[22] T. Yonezawa and N. Toshima, "Mechanistic consideration of formation of polymer-protected nanoscopic bimetallic clusters," *Journal of the Chemical Society, Faraday Transactions*, vol. 91, no. 22, p. 4111, 1995.

[23] M. Zubris, R. B. King, H. Garmestani, and R. Tannenbaum, "FeCo nanoalloy formation by decomposition of their carbonyl precursors," *Journal of Materials Chemistry*, vol. 15, pp. 1277–1285, 2005.

[24] X. Tuaev, S. Rudi, V. Petkov, A. Hoell, and P. Strasser, "In situ study of atomic structure transformations of Pt-Ni nanoparticle catalysts during electrochemical potential cycling," *ACS Nano*, vol. 7, no. 7, pp. 5666–5674, 2013.

[25] D. Wang, Y. Yu, H. L. Xin et al., "Tuning oxygen reduction reaction activity via controllable dealloying: a model study of ordered Cu_3Pt/C intermetallic nanocatalysts," *Nano Letters*, vol. 12, no. 10, pp. 5230–5238, 2012.

[26] V. Abdelsayed, A. Aljarash, M. S. El-Shall, Z. A. Al Othman, and A. H. Alghamdi, "Microwave synthesis of bimetallic nanoalloys and CO oxidation on ceria-supported nanoalloys," *Chemistry of Materials*, vol. 21, no. 13, pp. 2825–2834, 2009.

[27] C.-T. Hsieh, P.-Y. Yu, D.-Y. Tzou, J.-P. Hsu, and Y.-R. Chiu, "Bimetallic Pd-Rh nanoparticles onto reduced graphene oxide nanosheets as electrocatalysts for methanol oxidation," *Journal of Electroanalytical Chemistry*, vol. 761, pp. 28–36, 2016.

[28] R. Touroude, P. Girard, G. Maire, J. Kizling, M. Boutonnet-Kizling, and P. Stenius, "Preparation of colloidal platinum/palladium alloy particles from non-ionic microemulsions: characterization and catalytic behaviour," *Colloids and Surfaces*, vol. 67, pp. 9–19, 1992.

[29] G. Siné, D. Smida, M. Limat, G. Fóti, and C. Comninellis, "Microemulsion synthesized Pt/Ru/Sn nanoparticles on BDD for alcohol electro-oxidation," *Journal of the Electrochemical Society*, vol. 154, no. 2, pp. 170–178, 2007.

[30] J. Rymeš, G. Ehret, L. Hilaire, M. Boutonnet, and K. Jirátová, "Microemulsions in the preparation of highly active

combustion catalysts," *Catalysis Today*, vol. 75, no. 1–4, pp. 297–303, 2002.

[31] M. Ikeda, S. Takeshima, T. Tago, M. Kishida, and K. Wakabayashi, "Preparation of size-controlled Pt catalysts supported on alumina," *Catalysis Letters*, vol. 58, no. 4, pp. 195–197, 1999.

[32] I. Capek, "Preparation of metal nanoparticles in water-in-oil (w/o) microemulsions," *Advances in Colloid and Interface Science*, vol. 110, no. 1-2, pp. 49–74, 2004.

[33] C. Tojo, M. C. Blanco, and M. A. López-Quintela, "Preparation of nanoparticles in microemulsions: a Monte Carlo study of the influence of the synthesis variables†," *Langmuir*, vol. 13, no. 17, pp. 4527–4534, 1997.

[34] L. M. Magno, W. Sigle, P. A. van Aken, D. G. Angelescu, and C. Stubenrauch, "Microemulsions as reaction media for the synthesis of bimetallic nanoparticles: size and composition of particles," *Chemistry of Materials*, vol. 22, no. 23, pp. 6263–6271, 2010.

[35] W. Zhang, X. Qiao, and J. Chen, "Synthesis of silver nanoparticles—effects of concerned parameters in water/oil microemulsion," *Materials Science and Engineering: B*, vol. 142, no. 1, pp. 1–15, 2007.

[36] X. Zhang and K.-Y. Chan, "Water-in-Oil microemulsion synthesis of Platinum–Ruthenium nanoparticles, their characterization and electrocatalytic properties," *Chemistry of Materials*, vol. 15, no. 2, pp. 451–459, 2003.

[37] M.-L. Wu and L.-B. Lai, "Synthesis of Pt/Ag bimetallic nanoparticles in water-in-oil microemulsions," *Colloids and Surfaces A: Physicochemical and Engineering Aspects*, vol. 244, no. 1–3, pp. 149–157, 2004.

[38] P. Hernández-Fernández, S. Rojas, P. Ocón et al., "Influence of the preparation route of bimetallic Pt–Au nanoparticle electrocatalysts for the oxygen reduction reaction," *Journal of Physical Chemistry C*, vol. 111, no. 7, pp. 2913–2923, 2007.

[39] J. Eastoe, M. J. Hollamby, and L. Hudson, "Recent advances in nanoparticle synthesis with reversed micelles," *Advances in Colloid and Interface Science*, vol. 128–130, pp. 5–15, 2006.

[40] C.-H. Chen, L. S. Sarma, G.-R. Wang et al., "Formation of bimetallic Ag–Pd nanoclusters via the reaction between Ag nanoclusters and Pd^{2+} ions," *Journal of Physical Chemistry B*, vol. 110, no. 21, pp. 10287–10295, 2006.

[41] M.-L. Wu, D.-H. Chen, and T.-C. Huang, "Preparation of Au/Pt bimetallic nanoparticles in water-in-oil microemulsions," *Chemistry of Materials*, vol. 13, no. 2, pp. 599–606, 2001.

[42] R. M. Félix-Navarro, M. Beltrán-Gastélum, E. A. Reynoso-Soto, F. Paraguay-Delgado, G. Alonso-Nuñez, and J. R. Flores-Hernández, "Bimetallic Pt-Au nanoparticles supported on multi-wall carbon nanotubes as electrocatalysts for oxygen reduction," *Renewable Energy*, vol. 87, pp. 31–41, 2016.

[43] Y. Zhang, G. Chang, H. Shu, M. Oyama, X. Liu, and Y. He, "Synthesis of Pt-Pd bimetallic nanoparticles anchored on graphene for highly active methanol electro-oxidation," *Journal of Power Sources*, vol. 262, pp. 279–285, 2014.

[44] T. Szumełda, A. Drelinkiewicz, R. Kosydar, and J. Gurgul, "Hydrogenation of cinnamaldehyde in the presence of PdAu/C catalysts prepared by the reverse "water-in-oil" microemulsion method," *Applied Catalysis A: General*, vol. 487, pp. 1–15, 2014.

[45] M. Bonarowska, Z. Karpinski, R. Kosydar et al., "Hydrodechlorination using Pd–Au nanoparticles to convert chloro-containing compounds to useful chemicals," in *Reference Module in Materials Science and Materials Engineering*, Elsevier Inc., Amsterdam, Netherlands, 2016.

[46] Y. Hilli, N. M. Kinnunen, M. Suvanto, A. Savimäki, K. Kallinen, and T. A. Pakkanen, "Preparation and characterization of Pd-Ni bimetallic catalysts for CO and C_3H_6 oxidation under stoichiometric conditions," *Applied Catalysis A: General*, vol. 497, pp. 85–95, 2015.

[47] W. Weihua, T. Xuelin, C. Kai, and C. Gengyu, "Synthesis and characterization of Pt-Cu bimetallic alloy nanoparticles by reverse micelles method," *Colloids and Surfaces A: Physicochemical and Engineering Aspects*, vol. 273, no. 1–3, pp. 35–42, 2006.

[48] L. Xiong and A. Manthiram, "Nanostructured Pt-M/C (M=Fe and Co) catalysts prepared by a microemulsion method for oxygen reduction in proton exchange membrane fuel cells," *Electrochimica Acta*, vol. 50, no. 11, pp. 2323–2329, 2005.

[49] Y. M. López-De Jesú, C. E. Johnson, J. R. Monnier, and C. T. Williams, "Selective hydrogenation of benzonitrile by alumina-supported Ir–Pd," *Topics in Catalysis*, vol. 53, no. 15–18, pp. 1132–1137, 2010.

[50] J. Li, G. Wu, N. Guan, and L. Li, "NO selective reduction by hydrogen over bimetallic Pd-Ir/TiO_2 catalyst," *Catalysis Communications*, vol. 24, pp. 38–43, 2012.

[51] X. Wang, Y. Tang, Y. Gao, and T. Lu, "Carbon-supported Pd-Ir catalyst as anodic catalyst in direct formic acid fuel cell," *Journal of Power Sources*, vol. 175, no. 2, pp. 784–788, 2008.

[52] J. Chen, J. Zhang, Y. Jiang et al., "Enhanced formic acid electro-oxidation reaction on ternary Pd-Ir-Cu/C catalyst," *Applied Surface Science*, vol. 357, pp. 994–999, 2015.

[53] J. Chen, Y. Li, Z. Gao et al., "Ultrahigh activity of Pd decorated Ir/C catalyst for formic acid electro-oxidation," *Electrochemistry Communications*, vol. 37, pp. 24–27, 2013.

[54] Y. Nakagawa, K. Takada, M. Tamura, and K. Tomishige, "Total hydrogenation of furfural and 5-hydroxymethylfurfural over supported Pd-Ir alloy catalyst," *ACS Catalysis*, vol. 4, no. 8, pp. 2718–2726, 2014.

[55] C. Zlotea, F. Morfin, T. S. Nguyen et al., "Nanoalloying bulk-immiscible iridium and palladium inhibits hydride formation and promotes catalytic performances," *Nanoscale*, vol. 6, no. 17, pp. 9955–9959, 2014.

[56] H. Yang, C. Huang, F. Yang, X. Yang, L. Du, and S. Liao, "Mesoporous silica nanoparticle supported PdIr bimetal catalyst for selective hydrogenation, and the significant promotional effect of Ir," *Applied Surface Science*, vol. 357, pp. 558–563, 2015.

[57] Y. R. Luo, *Comprehensive Handbook of Chemical Bond Energies*, CRC Press, Boca Raton, FL, USA, 2007, http://www.crcnetbase.com/isbn/9781420007282.

[58] B. Darvent, *Bond Dissociation Energies in Simple Molecules*, Hathi Trust Digital Library, U.S. National Bureau of Standards, Gaithersburg, MD, USA, February 2016, http://catalog.hathitrust.org/Record/006255861.

[59] X. Yang, D. Chen, S. Liao et al., "High-performance Pd-Au bimetallic catalyst with mesoporous silica nanoparticles as support and its catalysis of cinnamaldehyde hydrogenation," *Journal of Catalysis*, vol. 291, pp. 36–43, 2012.

[60] L. J. Malobela, J. Heveling, W. G. Augustyn, and L. M. Cele, "Nickel-cobalt on carbonaceous supports for the selective catalytic hydrogenation of cinnamaldehyde," *Industrial & Engineering Chemistry Research*, vol. 53, no. 36, pp. 13910–13919, 2014.

[61] K.-Q. Sun, Y.-C. Hong, G.-R. Zhang, and B.-Q. Xu, "Synergy between Pt and Au in Pt-on-Au nanostructures for chemoselective hydrogenation catalysis," *ACS Catalysis*, vol. 1, no. 10, pp. 1336–1346, 2011.

[62] M. Guisnet, J. Barrault, C. Bouchoule, D. Duprez, C. Montassier, and G. Pérot, "Heterogeneous catalysis and fine chemicals. Proceedings of an International Symposium," in *Studies in Surface Science and Catalysis*, Elsevier, Amsterdam, Netherlands, 1988.

[63] F. Mauriello, M. Armandi, B. Bonelli, B. Onida, and E. Garrone, "H-bonding of furan and its hydrogenated derivatives with the isolated hydroxyl of amorphous silica: an IR spectroscopic and thermodynamic study," *Journal of Physical Chemistry C*, vol. 114, no. 42, pp. 18233–18239, 2010.

[64] G. Li, L. Jiang, Q. Jiang, S. Wang, and G. Sun, "Preparation and characterization of PdxAgy/C electrocatalysts for ethanol electrooxidation reaction in alkaline media," *Electrochimica Acta*, vol. 56, no. 22, pp. 7703–7711, 2011.

[65] M. H. M. T. Assumpção, S. G. da Silva, R. F. B. De Souza et al., "Investigation of PdIr/C electrocatalysts as anode on the performance of direct ammonia fuel cell," *Journal of Power Sources*, vol. 268, pp. 129–136, 2014.

[66] S. Y. Shen, T. S. Zhao, and J. B. Xu, "Carbon-supported bimetallic PdIr catalysts for ethanol oxidation in alkaline media," *Electrochimica Acta*, vol. 55, no. 28, pp. 9179–9184, 2010.

[67] J. C. M. Silva, B. Anea, R. F. B. D. Souza et al., "Ethanol oxidation reaction on IrPtSn/C electrocatalysts with low Pt content," *Journal of the Brazilian Chemical Society*, vol. 24, no. 10, pp. 1553–1560, 2013.

[68] C. He, "Evaluation of platinum-based catalysts for methanol electro-oxidation in phosphoric acid electrolyte," *Journal of The Electrochemical Society*, vol. 144, no. 3, p. 970, 1997.

[69] T. Szumełda, A. Drelinkiewicz, R. Kosydar, M. Góral-Kurbiel, J. Gurgul, and D. Duraczyńska, "Formation of Pd-group VIII bimetallic nanoparticles by the "water-in-oil" microemulsion method," *Colloids and Surfaces A: Physicochemical and Engineering Aspects*, vol. 529, pp. 246–260, 2017.

[70] L. M. Liz-Marzán and I. Lado-Touriño, "Reduction and stabilization of silver nanoparticles in ethanol by nonionic surfactants," *Langmuir*, vol. 12, no. 15, pp. 3585–3589, 1996.

[71] E. E. Finney and R. G. Finke, "Nanocluster nucleation and growth kinetic and mechanistic studies: a review emphasizing transition-metal nanoclusters," *Journal of Colloid and Interface Science*, vol. 317, no. 2, pp. 351–374, 2008.

[72] K. Hubkowska, U. Koss, M. Łukaszewski, and A. Czerwiński, "Hydrogen electrosorption into Pd-rich Pd-Ru alloys," *Journal of Electroanalytical Chemistry*, vol. 704, pp. 10–18, 2013.

[73] M. Łukaszewski and A. Czerwiński, "Selected electrochemical properties of Pd–Au alloys: hydrogen absorption and surface oxidation," *Journal of Solid State Electrochemistry*, vol. 12, no. 12, pp. 1589–1598, 2008.

[74] M. Łukaszewski, A. Żurowski, M. Grdeń, and A. Czerwiński, "Correlations between hydrogen electrosorption properties and composition of Pd-noble metal alloys," *Electrochemistry Communications*, vol. 9, no. 4, pp. 671–676, 2007.

[75] H. Duncan and A. Lasia, "Separation of hydrogen adsorption and absorption on Pd thin films," *Electrochimica Acta*, vol. 53, no. 23, pp. 6845–6850, 2008.

[76] R. Pattabiraman, "Electrochemical investigations on carbon supported palladium catalysts," *Applied Catalysis A: General*, vol. 153, no. 1-2, pp. 9–20, 1997.

[77] D. Rand and R. Woods, "Determination of the surface composition of smooth noble metal alloys by cyclic voltammetry," *Journal of Electroanalytical Chemistry*, vol. 36, no. 1, pp. 57–69, 1972.

[78] M. Simões, S. Baranton, and C. Coutanceau, "Electrooxidation of sodium borohydride at Pd, Au, and Pd_xAu_{1-x} carbon-supported nanocatalysts," *Journal of Physical Chemistry C*, vol. 113, no. 30, pp. 13369–13376, 2009.

[79] S. Lankiang, M. Chiwata, S. Baranton, H. Uchida, and C. Coutanceau, "Oxygen reduction reaction at binary and ternary nanocatalysts based on Pt, Pd and Au," *Electrochimica Acta*, vol. 182, pp. 131–142, 2015.

[80] C. Tojo, D. Buceta, and M. A. López-Quintela, "Understanding the metal distribution in core-shell nanoparticles prepared in micellar media," *Nanoscale Research Letters*, vol. 10, no. 1, p. 339, 2015.

[81] F. Barroso and C. Tojo, "Modelling of nano-alloying and structural evolution of bimetallic core-shell nanoparticles obtained via the microemulsion route," *Journal of Colloid and Interface Science*, vol. 363, no. 1, pp. 73–83, 2011.

[82] J. N. Solanki and Z. V. P. Murthy, "Controlled size silver nanoparticles synthesis with water-in-oil microemulsion method: a topical review," *Industrial & Engineering Chemistry Research*, vol. 50, no. 22, pp. 12311–12323, 2011.

[83] C. Tojo, D. Buceta, and M. A. López-Quintela, "Bimetallic nanoparticles synthesized in microemulsions: a computer simulation study on relationship between kinetics and metal segregation," *Journal of Colloid and Interface Science*, vol. 510, pp. 152–161, 2018.

[84] C. Tojo, F. Barroso, and M. de Dios, "Critical nucleus size effects on nanoparticle formation in microemulsions: a comparison study between experimental and simulation results," *Journal of Colloid and Interface Science*, vol. 296, no. 2, pp. 591–598, 2006.

[85] L. Zhang, J. M. Winterbottom, A. P. Boyes, and S. Raymahasay, "Studies on the hydrogenation of cinnamaldehyde over Pd/C catalysts," *Journal of Chemical Technology & Biotechnology*, vol. 72, no. 3, pp. 264–272, 1998.

[86] A. Giroir-Fendler, D. Richard, and P. Gallezot, "Selectivity in cinnamaldehyde hydrogenation of group-VIII metals supported on graphite and carbon," in *Studies in Surface Science and Catalysis*, vol. 41, pp. 171–178, Elsevier, Amsterdam, Netherlands, 1988.

[87] J. Long, H. Liu, S. Wu, S. Liao, and Y. Li, "Selective oxidation of saturated hydrocarbons using Au-Pd alloy nanoparticles supported on metal-organic frameworks," *ACS Catalysis*, vol. 3, no. 4, pp. 647–654, 2013.

[88] C. Tojo, M. de Dios, and M. A. López-Quintela, "On the structure of bimetallic nanoparticles synthesized in microemulsions," *Journal of Physical Chemistry C*, vol. 113, no. 44, pp. 19145–19154, 2009.